https://doi.org/10.7840/kics.2023.48.5.531

Performance Evaluation for UAV-Based UL-NOMA with Channel Coding

Hye Yeong Lee◆, Man Hee Lee*, Soo Young Shin°

ABSTRACT

Non-orthogonal multiple access is a potential technique to improve the spectral efficiency of beyond-5G systems by superposing multiple signals. For a received signal to be decoded, successive interference cancellation (SIC) process is required to subtract other signals at the receiver side. The channel coding is required to reduce the error probability when mobility is considered in non-orthogonal multiple access (NOMA) and applied after the SIC process. In this paper, we evaluate the performance of the unmanned aerial vehicle-based uplink NOMA with the concatenation of Reed - Solomon and convolutional code. Simulation results show comparisons between different conditions such as perfect and imperfect SIC processes.

Key Words : B5G wireless communication, non-orthogonal multiple access (NOMA), unmanned aerial vehicle (UAV), uplink, channel coding, bit error rate (BER)

Ⅰ. Introduction

Fifth-generation (5G) technology has been the first communication technology that attempted to systematically integrate and support all types of connected and automated mobility[1]. In addition, the 5G design of communication systems has led to the deployment of advanced systems to achieve improved spectrum efficiency, energy efficiency, quality of service (QoS), and reliability. In the future, new types of mobile devices will extend the uninterrupted coverage of the connectivity infrastructure and increase the density of connected devices.

To enhance the overall spectral efficiency, non-orthogonal multiple access (NOMA) is a predominant technology that superposes signals with different power coefficients, where a single-frequency resource is provided to multiple users[2,3]. The performance of NOMA overwhelms that of conventional orthogonal multiple access (OMA) because it serves multiple users at the same time and frequency and mitigates interference by applying the successive interference cancellation (SIC) process.

Owing to these advantages, NOMA has recently been extended to non-terrestrial networks (NTNs) such as unmanned aerial vehicles (UAVs), high-altitude platforms (HAPs), and satellite networks[4]. In particular, a UAV has many different requirements such as being efficient, secure, inclusive, and smart. Because a UAV provides the

※ This research was supported by the MSIT(Ministry of Science and ICT), Korea, under the ICAN(ICT Challenge and Advanced Network of HRD) program(IITP-2022-RS-2022-00156394) supervised by the IITP(Institute of Information & Communications Technology Planning & Evaluation)
※ This research was supported by Basic Science Research Program through the National Research Foundation of Korea (NRF) funded by the Ministry of Education (No. 2022R1I1A1A01066178)
◆ First Author : ICT Convergence Research Center, Kumoh National Institute of Technology, lhy413@kumoh.ac.kr, 정회원
° Corresponding Author : Kumoh National Institute of Technology, Department of IT Convergence Engineering, wdragon@kumoh.ac.kr, 종신회원
* Kumoh National Institute of Technology, Department of IT Convergence Engineering, fordmore@kumoh.ac.kr, 학생회원
논문번호 : 202302-024-A-RN, Received February 8, 2023; Revised April 7, 2023; Accepted April 20, 2023

potential for connectivity between many devices, it contributes to extending the communication range and exchange of massive amounts of information. In addition, it can act as a bridge between satellites and ground terminals. Therefore, several studies have been conducted on UAV-based downlink NOMA (DL-NOMA).

Unlike DL-NOMA, in uplink NOMA (UL-NOMA), each user decides to transmit a signal with its own assigned transmit power. This is because the maximum transmission power is limited by the user's battery capacity[5]. It is crucial for the superposed signal in UL-NOMA to be distinct, because the channels of each user are different from those in DL-NOMA. Interference from multiple users affects weak channel users because the base station (BS) receives signals simultaneously. Consequently, the SIC process performance is critical for weak channel users.

Generally, two SIC processes have been suggested: symbol-level and codeword-level SIC. The main difference between the two is that codeword-level SIC includes channel coding and decoding, that is, error correction. Therefore, codeword-level SIC can achieve a better bit error rate (BER) performance than symbol-level SIC[6].

Among the error corrections, the Reed–Solomon (RS) code has been employed in satellite communication for NTNs[7]. The RS code is a burst error-correcting code because of the use of multibit symbols rather than individual bits to encode data. However, the error cannot be corrected using single-error correction. Thus, a concatenated error correction was presented in [8] for reliable data transmission in a code division multiple-access system. This error correction employs both RS and convolutional codes.

In this study, we evaluated the performance of a UAV-based UL-NOMA with the concatenation of RS and convolutional code (RSCC). The simulation results included a BER comparison between OMA and NOMA and the application of RSCC. To validate the performance of the SIC process, we considered perfect and imperfect conditions for the coded UL-NOMA with $\mathcal{M}$-ary phase-shift keying (PSK) for modulation.

The remainder of this paper is organized as follows: Section 2 describes the proposed system and channel models. The RSCC-applied codeword-level SIC receiver is presented in Section 3. In Section 4, the simulation results are presented to compare the performances in terms of the BER. Finally, the conclusions of this study are presented in Section 5.

Ⅱ. System Model

The system model consists of a UAV and total K number of users, as shown in Fig. 1. Let us assume that the total number of users is divided into M near users and $(K-M)$ far users. The number of near and far users is equal to $(M=K/2)$ and M pairings are generated between a single near user and a single far user.

Following NOMA pairing, multiple users can superpose their signals on the same frequency resource at distinct power allocation levels. The transmission distance is limited to $d_k < d_{max}$. The pairings are compromised in the order of channel gains, $\sum_{m=1}^{M} |h_m|^2 > \sum_{k=M-K+1}^{K} |h_k|^2$. The channel gain can be a criterion for dividing near and far users and calculating the performance of UL-NOMA from the signal model, which is discussed later.

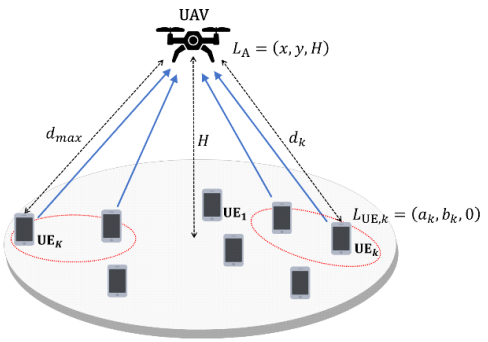

Fig. 1. UAV based UL-NOMA System

2.1 Transceiver design

The main structure of the UL-NOMA transceiver is shown in Fig. 2. Every user can transmit its or

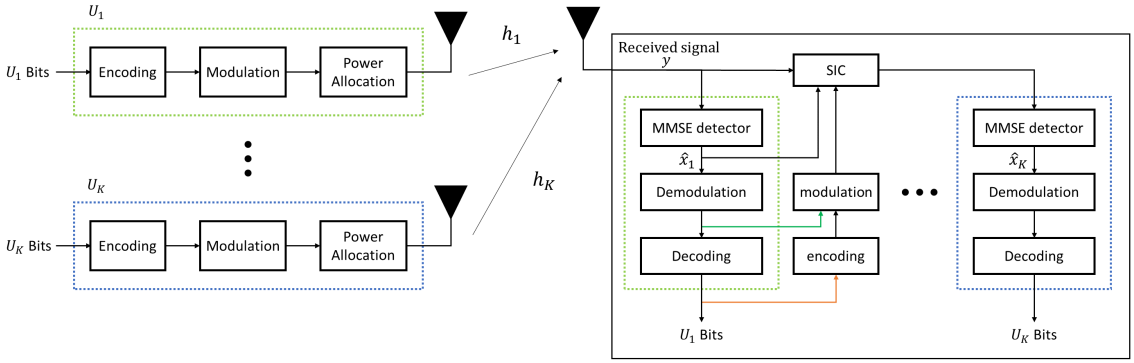

Fig. 2. Transceiver system model for UAV-based UL-NOMA with channel coding

own signal to the BS through a distinct channel and has an equivalent antenna. The transmitter consists of three parts: channel encoding, modulation, and power allocation. In this paper, the concatenated RSCC is utilized for error correction. Two encoders are used: inner convolution and outer RS codes. The convolutional code can be defined as CC (n, k, m), where n is the number of output bits, k is the number of input bits, and m is the length of the constraint. The code rate is k/n. The RS code is decomposed using RS (n, m), where n is the codeword length, and m is the number of bits per symbol. The codeword length is given by $n = 2^m - 1$.

At the BS, the receiver comprises a single antenna and four parts: the minimum mean-square error (MMSE) detector, demodulation, and the SIC process. In the RSCC decoder, scatter errors are corrected using the Viterbi decoder and burst errors are corrected using the RS decoder. Hence, the error propagation of coded NOMA can be dramatically reduced compared with that of uncoded NOMA.

2.2 Signal model

This paper considers a UL-NOMA scenario with multiple users and a BS. Users superpose different signals with distinct power levels on different channels. The location of the k-th user is denoted by the 3D Cartesian coordinates $L_{\mathrm{UE},k} = (a_k, b_k, 0)$ and the location of the UAV is denoted by LA = (x, y, H). The locations of the users and UAV are shown in Fig. 1. The Euclidean distance between the UAV and the k-th user is expressed as follows:

$$d_k = ((\mathrm{x} - a_k)^2 + (\mathrm{y} - b_k)^2 + H^2)^{1/2} \quad (1)$$

Generally, air-to-ground links are widely used in line-of-sight (LoS) and non-LoS (NLoS) channel models. In this paper, a Rician fading channel is assumed for the UL-NOMA system to consider both LoS and NLoS channels. The channel between the UAV and k-th user can be denoted as

$$h_k = \sqrt{\beta_k} g_k, \quad (2)$$

where β_k is the large-scale channel power gain given by $\beta_k = d_k^{-v}$ with pathloss v. g_k is the small-scale fading coefficient, expressed as

$$g_k = \sqrt{\frac{\mathcal{K}_k}{\mathcal{K}_k+1}} g + \sqrt{\frac{1}{\mathcal{K}_k+1}} \tilde{g}, \quad (3)$$

where g is the LoS channel component with $|g| = 1$, $\tilde{g}$ is the NLoS channel component, and $\mathcal{K}_k$ is the Rician factor. Adopting the equations in [9,10], the angle-dependent Rician factor can be defined as

$$\mathcal{K}_k = A_1 \exp(A_2 \theta_k), \quad (4)$$

where A_1 and A_2 are constant coefficients. Here, we set the Rician factor as $\mathcal{K}_{min} \le \mathcal{K}_k \le \mathcal{K}_{max}$ where $\mathcal{K}_{min} = A_1$ and $\mathcal{K}_{max} = A_2 \exp(A_2 \pi/2)$[10]. θ_k denotes the elevation angle given by $\theta_k = \arcsin(H / d_k)$.

Without loss of generality, let two users create a pairing to superpose the signals for the near and far users. The superposed signal of the near and far

users is given as follows:

$$x = \sum_{m=1}^{M} \sqrt{p_m} x_m + \sum_{k=M-K+1}^{K} \sqrt{p_k} x_k, \quad (5)$$

where x_m and x_k represent the messages from M near users and (K-M) far users, respectively. p_m and p_k denote the transmission power based on the user's condition.

The received signal at the BS is given as follows:

$$y = \sum_{k=1}^{K} \{h_k \circ x\} + w, \quad (6)$$

where w denotes Gaussian noise with zero mean and unit variance, and $\circ$ denotes the Hadamard product, which is known as the element-wise product.

Ⅲ. SIC Receiver in UL-NOMA

3.1 Perfect and Imperfect SIC

We highlight UL-NOMA challenges, such as SIC errors and channel coding. The performance of NOMA depends on perfect SIC to avoid strong interference signals. Consequently, an imperfect SIC is applied to the superposed signal, and the subtracted signal may also be an error.

The channel state information (CSI) for each user should be perfect, and measured CSI can be ordered such as $|h_1| > |h_2| \cdots > |h_M| > |h_{M-K+1}| > \cdots > |h_K|$.

The near users' signal detection applying MMSE receiver can be expressed as follows

$$\begin{aligned} \hat{x}_k &= y/h_k \\ &= \sqrt{p_k} x_k + (1/h_k) \sum_{j=1}^{M-K-k} h_j \sqrt{p_j} x_j + \widetilde{w}, \end{aligned} \quad (7)$$

where $\widetilde{w} = w/h_k$.

Generally, perfect and imperfect SIC are applied to far users to decode near user's signals. The far user's signal detection is expressed as follows:

$$\begin{aligned} \hat{x}_{M-K+k} &= y - h_k \sqrt{p_k} \hat{x}_k \\ &= h_k \sqrt{p_k} (x_k - \hat{x}_k) + \sum_{j=1}^{M-K+k} h_j \sqrt{p_j} x_j + w, \end{aligned} \quad (8)$$

where the case for $x_k = \hat{x}_k$ is perfect SIC and that for $x_k \neq \hat{x}_k$ is imperfect SIC.

3.2 Upper bound of error probability

We formulate a performance upper bound of the coded BER for a far user with perfect SIC. For the convolutional code with hard decision decoding, the performance upper bound of the coded BER after the Viterbi decoder is given by[11]

$$P_c < \sum_{d=d_{\text{free}}}^{\infty} \alpha_d P_e, \quad (9)$$

where d_{free} represents the free distance of the convolutional code. α_d is the total number of paths of distance d from the all-zero path that merges with the all-zero path for the first time[11]. P_e denotes the theoretical BER for $\mathcal{M}$-PSK with a Rician fading channel, i.e., the uncoded bit error probability, which can be expressed as [12]

$$P_e = \frac{1}{\pi} \int_0^{(\mathcal{M}-1)\pi/\mathcal{M}} M_\gamma \left(-\frac{\sin^2\left(\frac{\pi}{\mathcal{M}}\right)}{2\sin^2\theta} \right) \mathrm{d}\theta, \quad (10)$$

where M_γ is the moment generating function, which is given by [12]

$$M_\gamma(s) = \frac{(1+\mathcal{K})}{(1+\mathcal{K})-s\bar{\gamma}} \mathrm{e}^{\left[\frac{\mathcal{K}s\bar{\gamma}}{1+\mathcal{K}-s\bar{\gamma}}\right]}, \quad (11)$$

where $\bar{\gamma}$ is the average SNR per bit. For RS codes, the probability of a bit error at the output of the RS decoder can be upper-bounded as [8]

$$P_r < \sum_{i=t+1}^{n} \frac{i+t}{n} \binom{n}{t+1} P_b^i (1-P_b)^{n-i}, \quad (12)$$

where P_b is the m-bit symbol error probability. For RSCC, the simple upper bound for P_b is given by [13]

$$P_b < mP_c. \quad (13)$$

Ⅳ. Numerical Results

This section presents the performance evaluations of the proposed RSCC-based UL-NOMA under both perfect and imperfect SIC scenarios and compares it with the OMA system. In this study, we set the simulation parameters as listed in Table 1. We

Table 1. Simulation parameters

Parameter	Value
Number of users, K	2
Normalized distance range between UE_k and BS, d_k	[0.1, 1]
Normalized transmit power of UE_k, p_k	≤ 1.0
Modulation type	BPSK, QPSK
Antenna configuration	1× 1
Path loss exponent, v	4

considered the Rician factor $\mathcal{K}$ to be 8. For channel coding, a convolutional code was used as the inner code with a restriction length of 7 and a code rate of 1/2, whereas the RS code was used as an external code with a codeword length n of 7 and message length m of 3 as RS(7,3), where the parity length was $2t = (n - m) = 4$.

Fig. 3 compares the simulated BER and upper bound for UE1 under perfect SIC with and without RSCC using the expressions in (12) for the coded case and (10) for the uncoded case. We set the transmit power $p_1 = 1$, and the modulation used was BPSK. The results for the uncoded case perfectly matched the entire SNR range. However, the coded bounds were tight in the high-SNR region.

Fig. 4 depicts the BER with respect to SNR for UE_2 comparison with and without RSCC, namely coded (C) and uncoded (UC), where modulation set as BPSK ($\mathcal{M} = 2$) and the SNR for UE_1 was SNR_1 = 8dB. The SNR of the OMA user was the same as

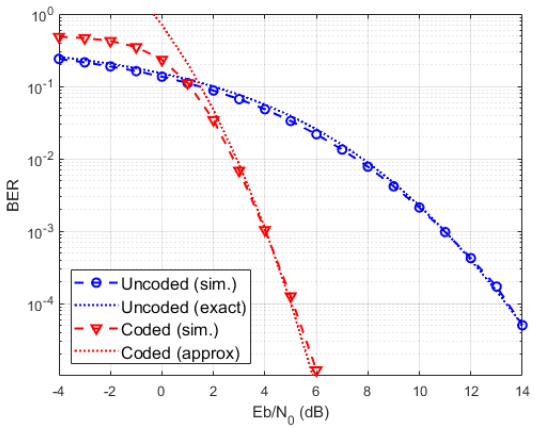

Fig. 3. Comparison of BER of UE_2: BPSK, pSIC

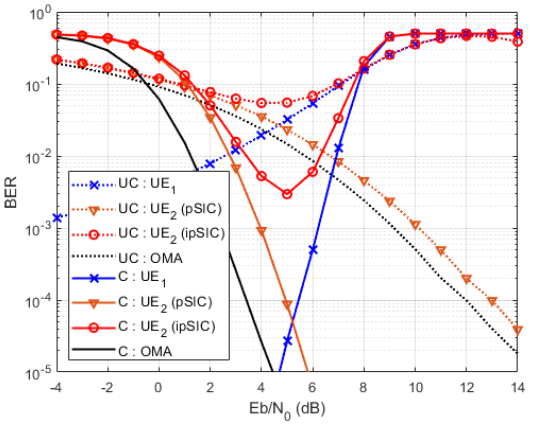

Fig. 4. Comparison of BER : BPSK, SNR_1 = 8dB

SNR_2. The normalized distance between users and the BS were $d_1 = 0.8$ and $d_2 = 1$, respectively. The transmit powers were $p_1 = 0.7$ and $p_2 = 1$. As shown in the figure, the difference in SNR between the two users affected the BER performance. As SNR_2 increased, the BER of UE_1 increased significantly because the interference from UE_2 to UE_1 increased as SNR_2 increased. The BER of UE_2 compared both perfect SIC (pSIC) and imperfect SIC (ipSIC) condition. Basically, with the increase in SNR_2 , the BER trend of UE_2 with perfect SIC was similar as that of OMA. In contrast, the BER of UE_2 with imperfect SIC decreased to the bottom at SNR_2 = 5dB and gradually increased again owing to the UE_1's error propagation[14]. Note that the trend was the same with and without RSCC. Based on that, the uncoded result for UE_1 performed better BER than the coded one in low SNR, whereas the coded result for UE_1 had a significantly better BER than the uncoded result because the number of occurrences of erroneous bits may have exceeded the error correction capability of RSCC code in lower SNR. In particular, the BER of UE_2 under imperfect SIC improved after RSCC coding.

Similarly, Fig. 5 compares the BER performances with and without RSCC when SNR_1 = 10dB. The other simulation parameters were set as shown in Fig. 4. As SNR_1 increased, the BER performance of the coded results further improved compared with that of the uncoded results.

Fig. 6 shows the BER performance using QPSK

($\mathcal{M}$ = 4), where SNR_1 = 10dB and the other parameters were the same as those in Fig. 5. In contrast to the BPSK results, the BER performance

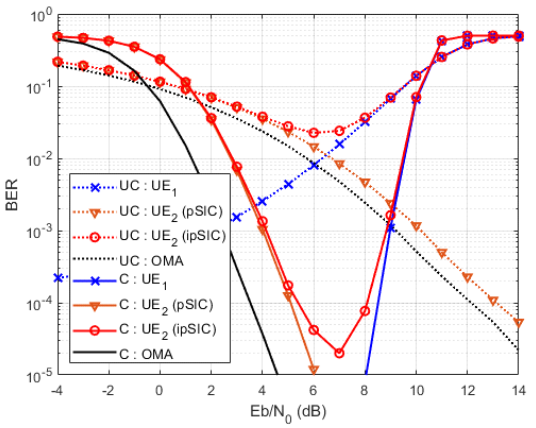

Fig. 5. Comparison of BER : BPSK, SNR_1 = 10dB

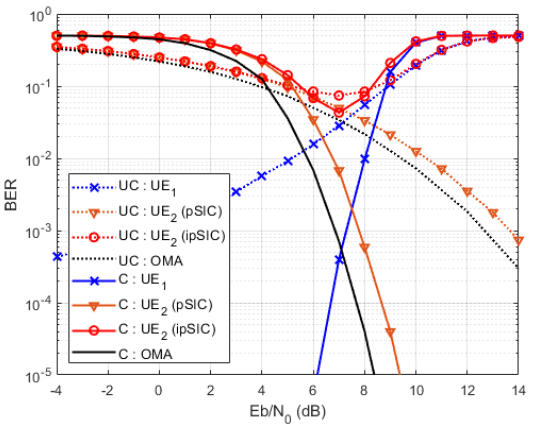

Fig. 6. Comparison of BER : QPSK, SNR_1 = 10dB

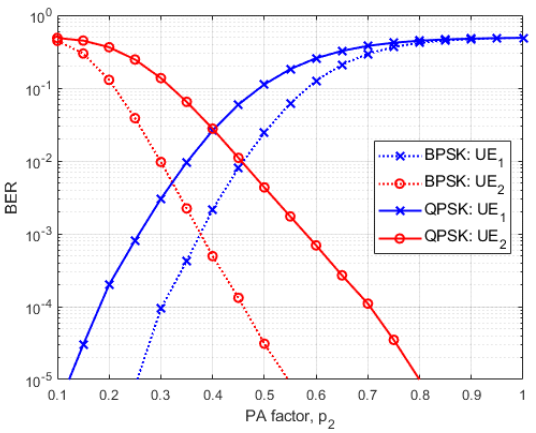

Fig. 7. Comparison of BER vs power factor

of a coded SIC had less performance improvement for an imperfect SIC.

Fig. 7 shows the BER with respect to the power allocation factor for UE_2. The power allocation factor varied p_2 varied as [0.1 1.0] and p_1 was fixed at 1.0. As shown in the figure, as the power factor increased, the BER for UE_2 improved.

V. Conclusion

In this study, we evaluated the performance of a UAV-based UL-NOMA system using a channel coding scheme. Here, the channel coding scheme considered was the concatenated Reed–Solomon and convolutional coding (RSCC). Moreover, we obtained the BER of UL-NOMA under perfect and imperfect SIC processes with different modulation orders. These results will be useful for integrating terrestrial and non-terrestrial networks in future studies.

References

[1] N. Panwar, S. Sharma, and A. K. Singh, "A survey on 5G: The next generation of mobile communication," *Phys. Commun.*, vol. 18, pp. 64-84, 2016. (https://doi.org/10.1016/j.phycom.2015.10.006)

[2] L. Dai, B. Wang, Z. Ding, Z. Wang, S. Chen, and L. Hanzo, "A survey of non-orthogonal multiple access for 5G," *IEEE Commun. Surv. & Tuts.*, vol. 20, no. 3, pp. 2294-2323, 2018. (https://doi.org/10.1109/COMST.2018.2835558)

[3] M. Ahmad, I N. A. Ramatryana, and S. Y. Shin, "NOMA and OMA comparison for multiple antenna technologies under high capacity constraints for 5g and beyond," *J. KICS*, vol. 45, no. 11, pp. 2004-2013, 2020. (https://doi.org/10.7840/kics.2020.45.11.2004)

[4] X. Zhu, C. Jiang, L. Kuang, N. Ge, and J. Lu, "Non-orthogonal multiple access based integrated terrestrial-satellite networks," *IEEE J. Sel. Areas in Commun.*, vol. 35, no. 10, pp. 2253-2267, 2017. (https://doi.org/10.1109/JSAC.2017.2724478)

[5] G. Geraci, et al., “What will the future of uav cellular communications be? a flight from 5G to 6G,” *IEEE Commun. Surv. & Tuts.*, vol. 24, no. 3, pp. 1304-1335, 2022. (https://doi.org/10.1109/COMST.2022.3171135)

[6] A. Khan, M. A. Usman, M. R. Usman, M. Ahmad, and S. Y. Shin, “Link and system-level NOMA simulator: The reproducibility of research,” *Electronics*, vol. 10, no. 19, p. 2388, 2021. (https://doi.org/10.3390/electronics10192388)

[7] W. Wu, D. Haccoun, R. Peile, and Y. Hirata, “Coding for satellite communication,” *IEEE J. Sel. Areas in Commun.*, vol. 5, no. 4, pp. 724-748, 1987. (https://doi.org/10.1109/JSAC.1987.1146583)

[8] R. D. Cideciyan, E. Eleftheriou, and M. Rupf, “Concatenated reed-solomon /convolutional coding for data transmission in CDMA-based cellular systems,” *IEEE Trans. Commun.*, vol. 45, no. 10, pp. 1291-1303, Oct. 1997. (https://doi.org/10.1109/26.634693)

[9] Iskandar and S. Shimamoto, “Channel characterization and performance evaluation of mobile communication employing stratospheric platforms,” *IEICE Trans. Commun.*, vol. 89, no. 3, pp. 937-944, Mar. 2006. (https://doi.org/10.1093/ietcom/e89-b.3.937)

[10] C. You and R. Zhang, “3D trajectory optimization in Rician fading for UAV-enabled data harvesting,” *IEEE Trans. Wireless Commun.,* vol. 18, no. 6, pp. 3192-3207, Jun. 2019. (https://doi.org/10.1109/TWC.2019.2911939)

[11] J. G. Proakis and M. Salehi, *Digital Communications*, vol. 4, New York: McGraw-hill, 2001.

[12] M. K. Simon and M.-S. Alouini, *Digital communication over fading channels*, New York: Wiley, 2001.

[13] M.-O. Wessman, A. Svensson, and E. Agrell, “Frequency diversity performance of coded multiband-OFDM systems on IEEE UWB channels,” *IEEE 60th VTC2004-Fall*, vol. 2, pp. 1197-1201, Los Angeles, CA, USA, 2004. (https://doi.org/10.1109/VETECF.2004.1400211)

[14] X. Wang, F. Labeau, and L. Mei, “Closed-form BER expressions of QPSK constellation for uplink non-orthogonal multiple access,” *IEEE Commun. Lett.*, vol. 21, no. 10, pp. 2242-2245, 2017. (https://doi.org/10.1109/LCOMM.2017.2720583)

Hye Yeong Lee

Feb. 2016 : B.S. degree, Kumoh National Institute of Technology

Feb. 2018 : M.S. degree, Kumoh National Institute of Technology

Feb. 2022 : Ph.D. degree, Kumoh National Institute of Technology

Mar. 2022~Current : Post Doc., ICT Convergence Research Center Kumoh National Institute of Technology

<Research Interests> 5G/6G wireless communications, signal processing

[ORCID:0000-0003-2924-4191]

Man Hee Lee

Feb. 2016 : B.S. degree, Kumoh National Institute of Technology

Feb. 2018 : M.S. degree, Kumoh National Institute of Technology

Mar. 2021~Current : Ph.D. student, Kumoh National Institute of Technology

<Research Interests> 5G/6G wireless communications, signal processing

[ORCID:0000-0003-1901-0279]

Soo Young Shin

Feb. 1999 : B.S. degree, Seoul National University
Feb. 2001 : M.S. degree, Seoul National University
Feb. 2006 : Ph.D. student, Seoul National University
Sep. 2010~Current : Professor, Kumoh National Institute of Technology

<Research Interests> 5G/6G wireless communications, Internet of things, drone applications

[ORCID:0000-0002-2526-2395]